



Angle resolved photoemission of single crystal SnO<sub>2</sub> using synchrotron radiation  
by Peter Leland Gobby

A thesis submitted in partial fulfillment of the requirements for the degree of DOCTOR OF PHILOSOPHY  
in Physics

Montana State University

© Copyright by Peter Leland Gobby (1977)

Abstract:

Polarization dependent angle-resolved ultraviolet photoemission (PARUPS) measurements have been performed on single crystal SnO<sub>2</sub>(001) using synchrotron radiation. Using photon energies up to 40 eV angle-integrated data revealed a total valence band width of approximately 9 eV, with a large density of states centered about 1.5 eV below the valence band maximum due to oxygen 2p states. A core level and its associated excitons were also investigated and have been interpreted as due to tin 4d levels.

Angle-resolved measurements allowed certain lower valence band structures to be emphasized which also showed strong polarization dependences. These structures have also been interpreted as due to tin 4d states. A covalent model was proposed which allowed this tin 4d character in both the observed core and the lower valence bands, though the two were separated by about 15 eV. Another initial state feature just above the valence band maximum was studied and has been interpreted as due to a large concentration of oxygen vacancies near the surface. It was felt that these vacancies were induced by annealing the crystal in vacuum.

ANGLE RESOLVED PHOTOEMISSION OF SINGLE CRYSTAL SnO<sub>2</sub>  
USING SYNCHROTRON RADIATION

by

PETER LELAND GOBBY

A thesis submitted in partial fulfillment  
of the requirements for the degree

of

DOCTOR OF PHILOSOPHY

in

Physics

Approved:

Gerald J. Lapuyse  
Chairperson, Graduate Committee

Robert J. Auer  
Head, Major Department

Henry L. Parsons  
Graduate Dean

MONTANA STATE UNIVERSITY  
Bozeman, Montana

May, 1977

## ACKNOWLEDGMENTS

The author is particularly grateful for the guidance and encouragement of his thesis advisor, Gerald J. Lapeyre. He would also like to thank John Hermanson for his hours of consultation on theoretical matters. Mark Baldwin, Cecil Badgley and Fred Blankenburg of the Montana State University Physics department and the staff of the University of Wisconsin Synchrotron Radiation Center have all provided much necessary technical help. Thanks also must go to C. G. Fonstad for supplying the crystals and to C. Olsen for allowing the use of his unpublished reflectance data. Finally, the author is indebted to the U. S. Air Force Office of Scientific Research, under grants No. AFOSR 71-2061 and 75-2872, for its financial support.

## TABLE OF CONTENTS

	Page
VITA . . . . .	ii
ACKNOWLEDGMENTS . . . . .	iii
LIST OF FIGURES . . . . .	vi
ABSTRACT . . . . .	x
I. INTRODUCTION . . . . .	1
II. SnO <sub>2</sub> BACKGROUND DATA . . . . .	5
A. Structure of Tin Oxide . . . . .	5
B. Survey of Tin Oxide Literature . . . . .	9
C. Tin Oxide - Ionic or Covalent? . . . . .	17
III. GENERAL THEORY . . . . .	25
A. Solid State Energy Levels . . . . .	25
B. Photoabsorption . . . . .	26
C. Selection Rules . . . . .	29
D. Inelastic Scattering . . . . .	32
E. Into the Vacuum . . . . .	33
IV. EXPERIMENTAL APPARATUS AND PROCEDURE . . . . .	35
A. Storage Ring Facility and Spectrometer . . . . .	35
B. Electron Energy Analyzer . . . . .	40
C. The Three Modes of Photoemission . . . . .	46
D. Sample Preparation . . . . .	53
1. Mounting and Cleaning . . . . .	53
2. Auger Analysis . . . . .	57

	Page
V. EXPERIMENTAL RESULTS AND DISCUSSION . . . . .	63
A. Angle-Integrated Study . . . . .	63
1. Valence Band Emission . . . . .	63
2. Primary Core Emission . . . . .	73
3. Core Excitons . . . . .	75
4. Discussion of the Atomic Origin of the Core . . . . .	86
B. Angle-Resolved Data . . . . .	90
1. General Angle-Resolved Techniques . . . . .	90
2. Normal Emission . . . . .	91
3. Extrinsic Emission . . . . .	92
4. "P"-polarization Data . . . . .	114
5. Non-normal Emission . . . . .	118
6. Lower Valence Bands Interpretation . . . . .	129
VI. SUMMARY . . . . .	138
APPENDICES . . . . .	143
A. Conservation of $\vec{k}_\parallel$ . . . . .	144
B. Derivation of Emission Angles as a Function of $\phi_D$ . . . . .	146
REFERENCES . . . . .	150

## LIST OF FIGURES

Figure	Page
1. SnO <sub>2</sub> unit cell. . . . .	6
2. Top view of SnO <sub>2</sub> (001) face. . . . .	7
3. SnO <sub>2</sub> Brillouin zone . . . . .	8
4. APW band calculation of SnO <sub>2</sub> . . . . .	10
5. KKR band structure calculation of SnO <sub>2</sub> . . . . .	11
6. Comparison of calculated SnO <sub>2</sub> energy levels . . . . .	13
7. SnO <sub>2</sub> reflectivity spectra . . . . .	16
8. A d <sup>2</sup> sp <sup>3</sup> hybrid orbital and its components . . . . .	21
9. Overlap of tin 4d and oxygen 2p radial wavefunctions. . . . .	24
10. Schematic of selection rules . . . . .	31
11. Storage rin schematic . . . . .	36
12. Schematic of experimental chamber . . . . .	37
13. Light and subsequent electron optics systems . . . . .	38
14. Light curve . . . . .	39
15. CMA electronics and data acquisition electronics . . . . .	41
16. Angle-resolving CMA . . . . .	44
17. Transmission of angle-resolving CMA . . . . .	45
18. Relative sample to light orientations for s and "p"-polarizations . . . . .	47
19. DOS and energy levels for hypothetical sample . . . . .	49
20. Idealized UPS spectra from hypothetical sample . . . . .	52

Figure	Page
21. Crystal holder. . . . .	55
22. AREDC's depicting sample preparation . . . . .	56
23. $\phi$ -patterns before and after annealing of crystal . . . . .	58
24. Atomic Auger process . . . . .	59
25. Characteristic Auger spectra from SnO <sub>2</sub> . . . . .	61
26. AIEDC's for $h\nu = 11.0$ to $15.5$ eV . . . . .	64
27. AIEDC's for $h\nu = 15.5$ to $19.0$ eV . . . . .	65
28. AIEDC's for $h\nu = 19.0$ to $25.0$ eV . . . . .	66
29. AIEDC's for $h\nu = 25.0$ to $31.0$ eV . . . . .	67
30. Comparison of calculated VBDOS to experiment . . . . .	69
31. AICIS's demonstrating CBDOS . . . . .	72
32. AIEDC's showing SnO <sub>2</sub> core . . . . .	74
33. AICFS's showing SnO <sub>2</sub> core . . . . .	76
34. AICFS's demonstrating exciton Auger decay . . . . .	78
35. Direct recombination and Auger decay modes of core exciton . . . . .	79
36. Predicted Auger distribution using experimental VBDOS . . . . .	81
37. AICIS's demonstrating DR enhancement . . . . .	83
38. AIEDC's at photon energies near and at exciton energy . . . . .	85
39. EDC's of metallic tin showing 4d core emission . . . . .	87
40. AICFS's on SnO <sub>2</sub> with Sn overlayer . . . . .	88
41. Normal emission AREDC's for $h\nu = 11.0$ to $16.5$ eV . . . . .	93

Figure	Page
42. Normal emission AREDC's for $h\nu = 16.5$ to $22.0$ eV . . .	94
43. Normal emission AREDC's for $h\nu = 22.0$ to $31.0$ eV . . .	95
44. AREDC's taken at $h\nu = 18.0$ eV, $\phi = \langle 100 \rangle$ . . . . .	97
45. EDC of $\text{SnO}_2$ with Sn overlayer showing emission at $E_F$ .	98
46. Graph of $E_F$ as a function of donor concentration . . .	100
47. $\text{SnO}_2$ absorption data . . . . .	105
48. Comparison of single crystal and oxidized film EDC's .	107
49. Comparison of metallic tin and oxidized tin EDC's . . .	109
50. EDC's showing tin 4d core in oxidized tin film . . . .	111
51. Oxygen vacancy defect "molecule" . . . . .	113
52. "P"-polarization normal emission EDC's for $h\nu = 11.0$ to $16.0$ eV . . . . .	115
53. "P"-polarization normal emission EDC's for $h\nu = 16.0$ to $21.0$ eV . . . . .	116
54. "P"-polarization normal emission EDC's for $h\nu = 21.0$ to $32.0$ eV . . . . .	117
55. "P"-polarization EDC's for $h\nu = 29.0$ eV, $\phi = \langle 100 \rangle$ . . .	119
56. $\text{SnO}_2$ $\phi$ -patterns . . . . .	121
57. ARCIS's for $E_i = -8.0$ eV . . . . .	122
58. S-polarization AREDC's for $h\nu = 28.0$ eV, $\theta = 20^\circ$ . . . .	125
59. S-polarization AREDC's for $h\nu = 28.0$ eV, $\phi = \langle 100 \rangle$ . . .	127
60. S-polarization AREDC's for $h\nu = 28.0$ eV, $\phi = \langle 110 \rangle$ . . .	128
61. S-polarization ARCFs's for $ k  = .94 \text{ \AA}^{-1}$ . . . . .	130



Figure	Page
62. Angular d-functions with octahedral coordination. . . .	134
63. Experimentally determined energy level diagram with interpreted atomic origins . . . . .	139
64. Schematic depicting relationship between the drum angle and the emission angle . . . . .	147
65. Graph of drum angle versus emission angle . . . . .	149

## ABSTRACT

Polarization dependent angle-resolved ultraviolet photoemission (PARUPS) measurements have been performed on single crystal  $\text{SnO}_2(001)$  using synchrotron radiation. Using photon energies up to 40 eV<sup>2</sup> angle-integrated data revealed a total valence band width of approximately 9 eV, with a large density of states centered about 1.5 eV below the valence band maximum due to oxygen 2p states. A core level and its associated excitons were also investigated and have been interpreted as due to tin 4d levels.

Angle-resolved measurements allowed certain lower valence band structures to be emphasized which also showed strong polarization dependences. These structures have also been interpreted as due to tin 4d states. A covalent model was proposed which allowed this tin 4d character in both the observed core and the lower valence bands, though the two were separated by about 15 eV. Another initial state feature just above the valence band maximum was studied and has been interpreted as due to a large concentration of oxygen vacancies near the surface. It was felt that these vacancies were induced by annealing the crystal in vacuum.

## I. INTRODUCTION

Since the pioneering work of Berglund and Spicer<sup>1</sup> less than 15 years ago, ultraviolet photoemission spectroscopy (UPS) has grown to be one of the leading tools of the solid-state physicist. Its appeal is two-fold. First the photon energy range of 1 - 50 eV used is in the range necessary to excite valence electrons and shallow core electrons into normally unoccupied states. It is these valence and shallow core electrons which contribute to molecular and crystal binding and are consequently of primary interest to the solid-state physicist. The second appeal lies in the fact that UPS is a double spectroscopy. That is, electron emission is determined as a function of the final energy of the electron as well as the photon energy. In contrast, a reflectance experiment, for example, is a single spectroscopy, since the reflectance is determined as a function of only the photon energy.

More recently, the availability of synchrotron radiation<sup>2</sup> with its intense continuum has made it practical to restrict the emission angle of the detected electron over a wide range of final energies. In effect, this allows one to measure the momentum as well as kinetic energy of the emitted electron. The polarized nature of the synchrotron radiation has also been utilized to help bring about polarization dependent angle-resolved photoemission. These studies have allowed

the determination of high densities of states in the electronic energy band structure of gallium arsenide<sup>3</sup> and tungsten<sup>4</sup> and, in the case of some two dimensional crystals<sup>5</sup> and surface states<sup>6,7</sup>, direct measurement of the total electronic energy bands.

Tin oxide provides an interesting challenge for this powerful tool. It is known to be a wide band gap ( $E_g \sim 3.5$  eV) semiconductor crystallizing in the rutile structure. Naturally occurring crystals are known as cassiterite. It is chemically inert, with a high melting point, perhaps as high as 2000°C.<sup>8</sup> Its most notable current use is as a transparent conducting film on airplane windows for purposes of defrosting.

Relatively little is known about the electronic structure of SnO<sub>2</sub> compared to, say, silicon, gallium arsenide, tungsten or even the alkali halides. Most experimental work has centered on electrical conductivity measurements<sup>9,10,11</sup> and optical studies<sup>12-18</sup> at or near the band gap. Conductivity experiments have particularly been hampered by a lack of good quality single crystals. Prior to this work, no photoemission work had been reported. Theoretical studies are few; this is due in part to the complicated rutile structure. There have been two band calculations reported in the literature, with values for the valence band widths of approximately 5 eV<sup>19</sup> and more than 10 eV<sup>20</sup>, respectively.

Furthering the understanding of SnO<sub>2</sub> - particularly its

electronic structure - can benefit two scientific groups: theoretical physicists and semiconductor device physicists. The benefits to the latter group are straightforward and uncomplicated. The search for rugged high temperature semiconductor devices remains in progress. Tin oxide, with its chemical inertness and wide band gap, definitely has potential in this regard. In a related vein, some work has been done on indium-tin oxide and antimony doped tin oxide films regarding selective surfaces for solar collectors.<sup>21</sup> Pertinent data on the electronic structure of tin oxide will be necessary to maximize the probability of success in these two areas.

Tin oxide should be interesting to theoretical physicists because of its lack of simplicity. The more standard semiconductors - silicon, germanium and gallium arsenide - have two simplifying things in common: cubic symmetry and predominantly covalent bonding using atomic s and p orbitals. The electronic structures of these materials consequently have a number of similarities. The calculated energy band structures have been checked against much experimental data and have fared well.<sup>3,4</sup> The band structure theorists have thus been able to check and adjust their calculation techniques for these materials and now can extend these techniques to similar materials with a high degree of confidence. But extension to tin oxide is not so straightforward. Evidence of this lies in the difference of the calculated band widths previously mentioned. The unit cell of tin oxide is

tetragonal instead of cubic, and the bonding is probably not well described as either covalent or ionic, but a strong mixture of the two. There is even evidence in this study of significant d as well as s and p atomic orbitals involved in the covalent aspect of the binding. Experimental data on more complicated systems such as tin oxide will allow the theoretical techniques to be advanced still further.

Pertinent data on the electronic structure of tin oxide have been acquired in this thesis project. Using photon energies up to 40 eV, the valence bands (VBs), lower conduction bands (CBs) and an atomic-like core level were studied. A structure lying just above the valence band maximum (VBM) was observed and has been interpreted as due to defects induced by sample preparation. Exclusion of this defect structure from the bulk VBs resulted in a total experimental VB width of ~9 eV. Angle-resolved measurements allowed some VB structures to be further emphasized, so that interpretation of their respective atomic origins was somewhat simplified. These data seem to indicate that bonding in  $\text{SnO}_2$  has strong covalent as well as ionic character.

## II. SnO<sub>2</sub> BACKGROUND DATA

### A. Structure of Tin Oxide

Tin oxide crystallizes in the rutile structure with space group  $D_{4h}^{14}$ .<sup>22</sup> The unit cell shown in Fig. 1 is simple tetragonal and contains two tin atoms and four oxygen atoms.  $a = b = 4.74 \text{ \AA}$ , while  $c = 3.19 \text{ \AA}$ , and the nearest neighbor oxygen-oxygen distance is  $2.54 \text{ \AA}$ .<sup>23</sup> With these x-ray diffraction data, it is then straightforward to calculate the remaining pertinent parameters.

Each tin atom is surrounded by an irregular octahedron of oxygens. The Sn-O distance is  $2.08 \text{ \AA}$  for those lying in an (001) plane and  $2.04 \text{ \AA}$  for the remaining four. The O-Sn-O "dumbbell" in the (001) plane is perpendicular to the plane containing the tin atom and the other four oxygen atoms. The acute angle between two adjacent oxygens with the tin atom at the vertex is  $77^\circ$ .

Another perspective of the tin oxide structure can be attained with the help of Fig. 2, a view of the (001) face of the crystal looking down the  $\vec{c}$  axis. The sizes of the tin and oxygen spheres correspond to their ionic radii -  $\text{Sn}^{4+}$  and  $\text{O}^{2-}$ , respectively.<sup>24</sup>

For completeness the Brillouin zone (BZ) for stannic oxide is shown in Fig. 3. The irreducible 1/16 zone is labeled with symmetry points and lines following the notation of Koster.<sup>25</sup>

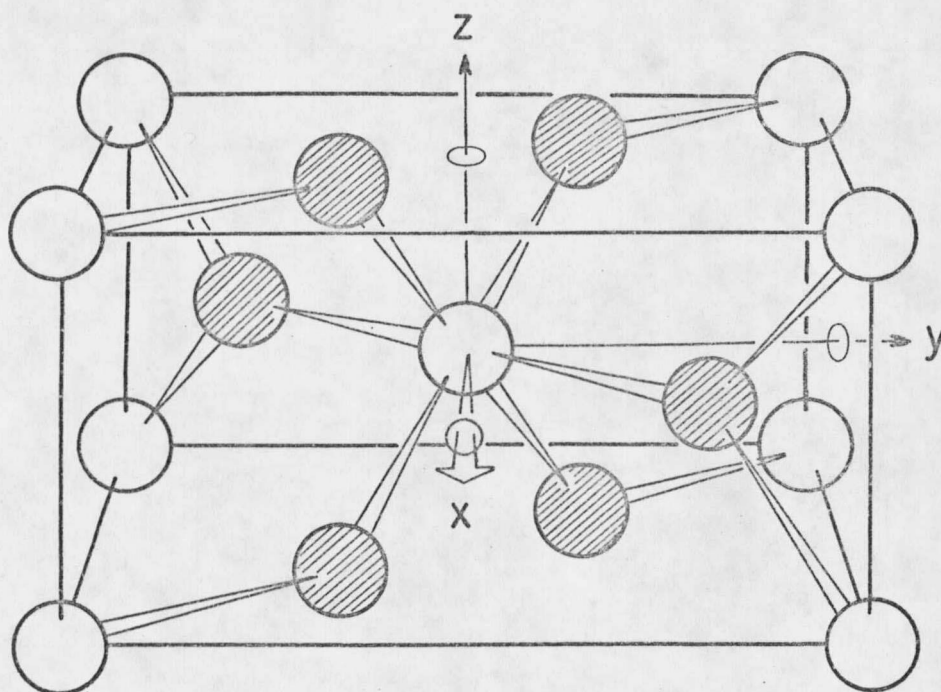


FIG. 1. SnO<sub>2</sub> unit cell. Shaded spheres represent the oxygen atoms.















































































































































































































































































































































